GEM TN-93-444
MIT-GEM-EM-20

Electromagnetic Field Distribution in the Lead Region of the SSC GEM Detector Based on a 12 Bobbin Winding Pack

R. L. Myatt
Plasma Fusion Center
Massachusetts Institute of Technology
Cambridge, MA

June 20, 1993

This document and all reports and memoranda in this series are intended as a record of work in progress. They are for use in informal discussions of design and fabrication alternatives. This material is subject to change and should not, therefore, be published or referred to in the open literature. Conclusions are preliminary and distribution should be strictly limited.

Abstract;

This magnetic field produced by the GEM detector magnet is quantified by a two-dimensional (2-D) axisymmetric ANSYS [1] model. The analysis takes advantage of symmetry in the split solenoid geometry and models the axisymmetric magnetic components associated with half of the detector: a 12-bobbin coil, a carbon steel vacuum vessel and a forward field shaper (FFS). The objective of this report is to present radial and axial flux density data in the region outside of the coil and inside the vacuum vessel wall. These data are to be used in the design and analysis of leads and joints. The analysis follows very closely the work presented in [2], with one significant change: the split solenoid is modeled more accurately as 12 discrete winding packs, instead of one coil within a 0.068 x 14.25 meter envelope. A separate study which models a single bobbin with 19 discrete conductor turns is used to confirm the adequacy of this approach. The study indicates that the field values at radii greater than the bobbin outside radius are the same, whether the winding is modeled as 19 turns with current running in the superconducting (SC) cable, or as a uniform current density averaged over the aluminum sheath and SC cable.

MIT-GEM-EM-20

Electromagnetic Field Distribution in the Lead Region of the SSC GEM Detector Based on a 12 Bobbin Winding Pack

July 20, 1993

R.L. Myatt

This document and all reports and memoranda in this series are intended as a record of work in progress. They are for use in informal discussions of design and fabrication alternatives. This material is subject to change and should not, therefore, be published or referred to in the open literature. Conclusions are preliminary and distribution should be strictly limited.

Plasma Fusion Center
Massachusetts Institute of Technology
Cambridge, MA 0213

MIT GEM DETECTOR Memoranda
Approval Sheet

B.A. Smith
Project Engineer

7/16/93
Date

R.D. Pillsbury, Jr.
Technical Manager

7/16/93
Date

A.M. Dawson
Technical Editor

Date

1.0 Abstract

The magnetic field produced by the GEM detector magnet is quantified by a two-dimensional (2-D) axisymmetric ANSYS [1] model. The analysis takes advantage of symmetry in the split solenoid geometry and models the axisymmetric magnetic components associated with half of the detector: a 12-bobbin coil, a carbon steel vacuum vessel and a forward field shaper (FFS). The objective of this report is to present radial and axial flux density data in the region outside of the coil and inside the vacuum vessel wall. These data are to be used in the design and analysis of leads and joints. The analysis follows very closely the work presented in [2], with one significant change: the split solenoid is modeled more accurately as 12 discrete winding packs, instead of one coil within a 0.068 x 14.25 meter envelope. A separate study which models a single bobbin with 19 discrete conductor turns is used to confirm the adequacy of this approach. The study indicates that the field values at radii greater than the bobbin outside radius are the same, whether the winding is modeled as 19 turns with current running in the superconducting (SC) cable, or as a uniform current density averaged over the aluminum sheath and SC cable.

2.0 Conclusions

The 2-D electromagnetic model of the GEM detector presented in [2] is refined to capture the field ripple caused by the discretization of the 12 bobbin coil. The refinement has no significant impact on the field beyond the vacuum vessel and, therefore, the flux density component plots presented in [2] still apply. However, the field within the envelope of the vacuum vessel is affected by the nonuniformity of the current distribution in the coil. The primary effect is caused by voids in the winding pack between bobbins, while the secondary effect is caused by voids between SC cables. Flux density component plots are presented and illustrate this local field ripple.

The analysis indicates that the peak-to-peak field ripple caused by the spacing between SC cables is about 0.11 and 0.02 tesla in the radial and axial fields, respectively, at the outer radius of the sheath (9.534 meters). And although this ripple diminishes completely within about 0.08 m of the sheath OD, the effect of the voids between bobbins is evident throughout the entire vacuum vessel envelope.

3.0 Analysis Methodology

The analysis methodology follows closely that which is outlined in [2]. However, the approach differs in the detail used to model the detector coil. In the original analysis the current is averaged over a uniform winding pack which has a mean radius of 9.5 m, a radial build of 0.068 m and an axial length of 14.25 m. An average current density is applied over this entire area to achieve an on-axis flux density of 0.8 tesla at the detector's vertical midplane. Although this simplification is adequate for field results outside of the vacuum vessel envelope, it does not adequately represent the field distribution close to the winding pack.

The baseline conductor is shown in Fig 3.0-1. Under normal operating conditions, current flows in the superconducting cable, which is contained within a 0.020 m ID conduit. Nineteen turns spaced 0.05236 m on center, make up a bobbin (Fig 3.0-2), and 12 bobbins make up one coil of the split solenoid pair (Fig 3.0-3). Bobbin assembly hardware disrupts this 0.05236 m center-to-center current spacing with about 0.190 m between the last turn in one bobbin and the first turn in the adjacent bobbin.

This report describes the two phases of the analysis. In the first phase, a detailed model of a single bobbin is used to determine the minimum current source definition necessary to capture the field close to the coil. These findings are used to define the appropriate current source in the 2-D

model of the detector. The refinement in the model provides good results within a small distance of the coil, which will be especially useful in the design and analysis of the coil's current leads.

3.1 Detailed Analyses of a Single Bobbin

Two finite element models of a single bobbin have been built for the purpose of determining the minimum level of detail necessary to estimate accurately the field in the region of the coil leads. In the more detailed model, the current carried by the bobbin's 19 turn, 0.020 m diameter superconducting cable is simulated by (19) 0.01772 m square elements on 0.05236 m centers, lying on a mean radius of 9.5 m. In the less-detailed model, the same amount of current is spread over the area occupied by the cable, sheath, and turn-to-turn insulation, with radial and axial builds of 0.0685 m and 0.9948 m, respectively, and a mean radius of 9.5 m. Both models include the vacuum vessel walls, the surrounding air, and boundary conditions which simulate an infinitely repeating geometry. This allows a great deal of detail to be used in the region of interest without having to model the entire detector.

Figures 3.1-1 and 3.1-2 show the coil and vacuum vessel walls, excluding air elements, for each of these single bobbin models. Although these models cannot be used to estimate the field distribution in the GEM detector, they can be used to capture the effects of the current source definition and show how quickly the results converge to the same solution with increasing distance from the winding.

3.2 Analysis of the GEM Detector

The results of the detailed single bobbin study described above led to a 2-D model of the GEM detector which adequately estimates the field within a small distance of the coil. In essence, the model developed in [2] is modified to account for the discreteness of the 12-bobbin coil. The mesh is refined in the axial direction such that the element size is on the order of a conductor width. Plots of the model are shown in Figs 3.2-1 and 3.2-2. Air elements are excluded from the plot to highlight the coil and magnetic steel components.

4.0 Results

4.1 Results of the Single Bobbin Study

The results of the single bobbin analysis are summarized in a series of field component path plots along the length of the model. Figure 4.1-1 shows these field components at a radius of 9.534 m (along the outside radius of the sheath) for the detailed model. The ripple in the flux density plot (±0.055 tesla about the mean value for the radial component and ±0.010 tesla about the mean value for the axial component) indicates the presence of spacing between the 19 SC cables. Figure 4.1-2 shows similar data for the case in which the current is distributed over the entire sheath and SC cable area. Like the distribution of currents, the curves are smooth and appear to represent the mean value of the rippled curves shown earlier for the discrete current source model.

A similar pair of plots is shown for the results at a radius of 9.617 m, which is essentially the outside radius of the bobbin. Figure 4.1-3 shows that the ripple caused by the individual conductor sources has essentially disappeared, and the values compare very closely with the distributed current case shown in Fig 4.1-4.

These results conclude that modeling a uniform current density over the sheath and SC cable area is adequate for estimating the field in regions beyond the outside radius of the bobbin. Closer to the coil, a ripple in the field occurs and the uniform current model does not accurately

represent this behavior.

4.2 Results of the Full GEM Detector Field Analysis

The revised model produces detailed field results which capture the effects of conductor spacing between bobbins. As concluded in section 4.1, the effects of the SC cable spacing attenuate within about 0.08 m, and are not significant in the region of the leads.

Results are characterized by the contours of constant flux shown in Fig 4.2-1, and the flux density component path plots shown in Figs 4.2-2 to 4.2-7. While the flux contour plot provides a qualitative picture of the flux path in the region of the detector, the path plots provide useful numerical results in the form of radial and axial flux density data in free space at various radial positions. Each path begins at the symmetry plane (Y=0) and extends along a constant radius path, ending 0.1 meters past the winding pack (Y=15). Breaks in each curve occur at an axial position of 0.4 meters, where the path crosses through the iron flange.

An additional plot, Fig 4.2-8, is included which shows the axial and radial flux density distributions at a radius of 9.534 m. Although the field ripple caused by the discrete SC cable spacing is not produced by this model, this approximate result is of value in estimating the field in the region of the bobbin-to-bobbin joints. It is interesting to note that very similar results were found at this radius with a linear model, assuming no FFS or vacuum vessel, indicating that within close proximity to the current source, the iron vacuum vessel and FFS have little effect on the field.

5.0 References

1. ANSYS 5.0, Swanson Analysis Systems, Inc., Houston, PA

2. R.L. Myatt, "Electromagnetic Field Distribution in the Region of the Coil Leads of the SSC GEM Detector," MIT-GEM-EM-12, Nov. 10, 1992, MIT Plasma Fusion Center, Cambridge, MA

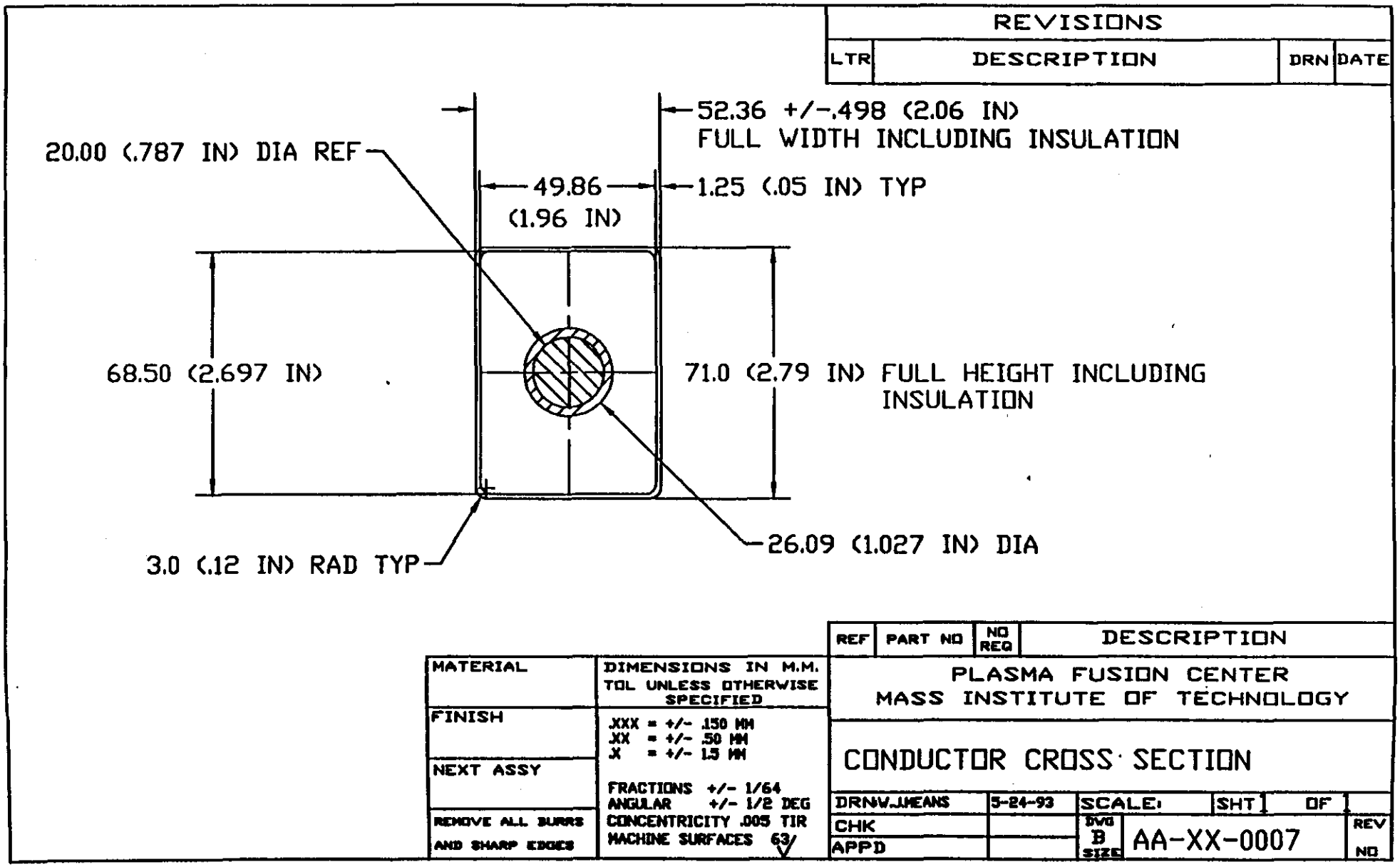

Fig 3.0-1 Conductor Cross Section

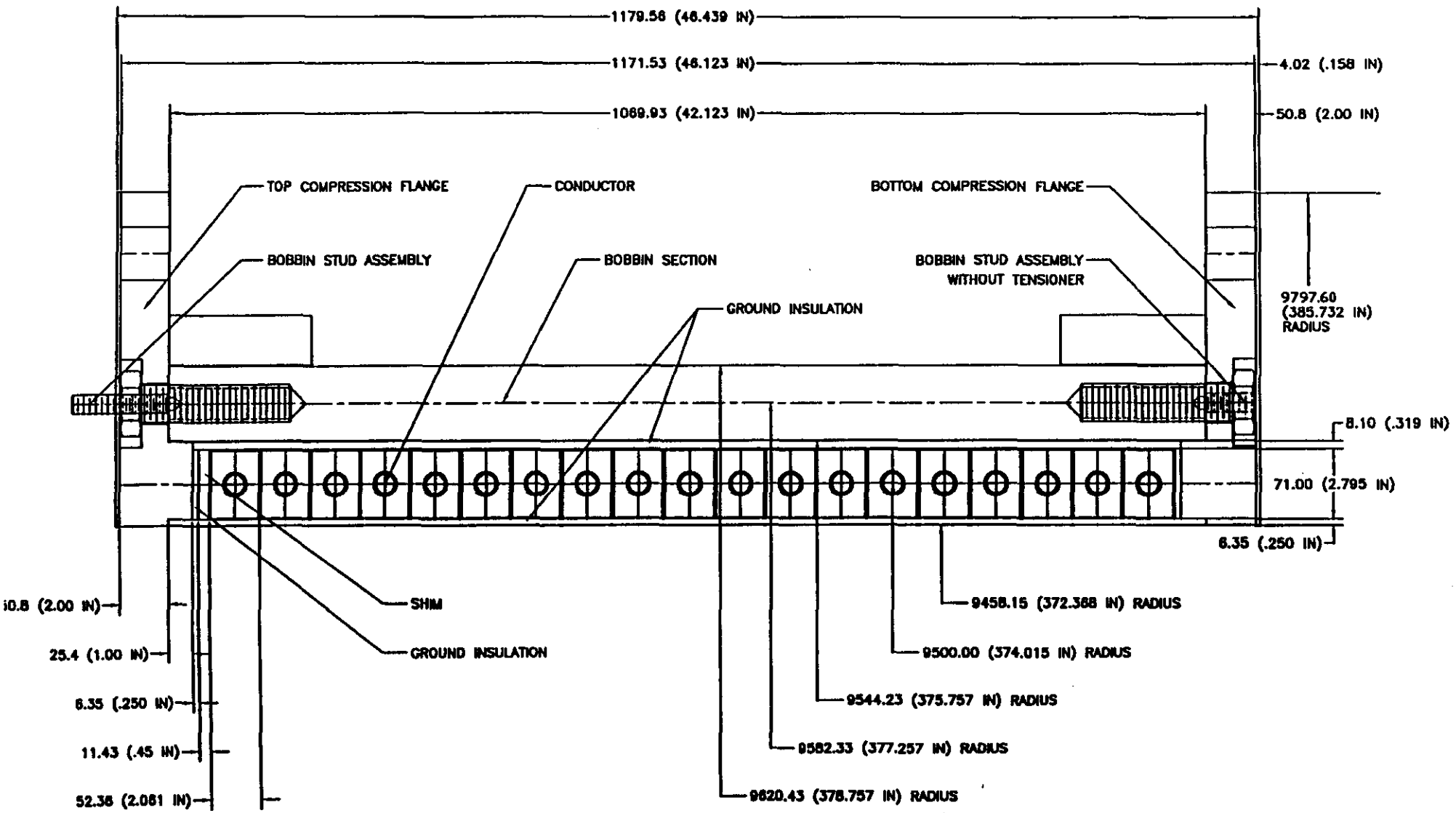

Fig 3.0-2 Bobbin Cross Section

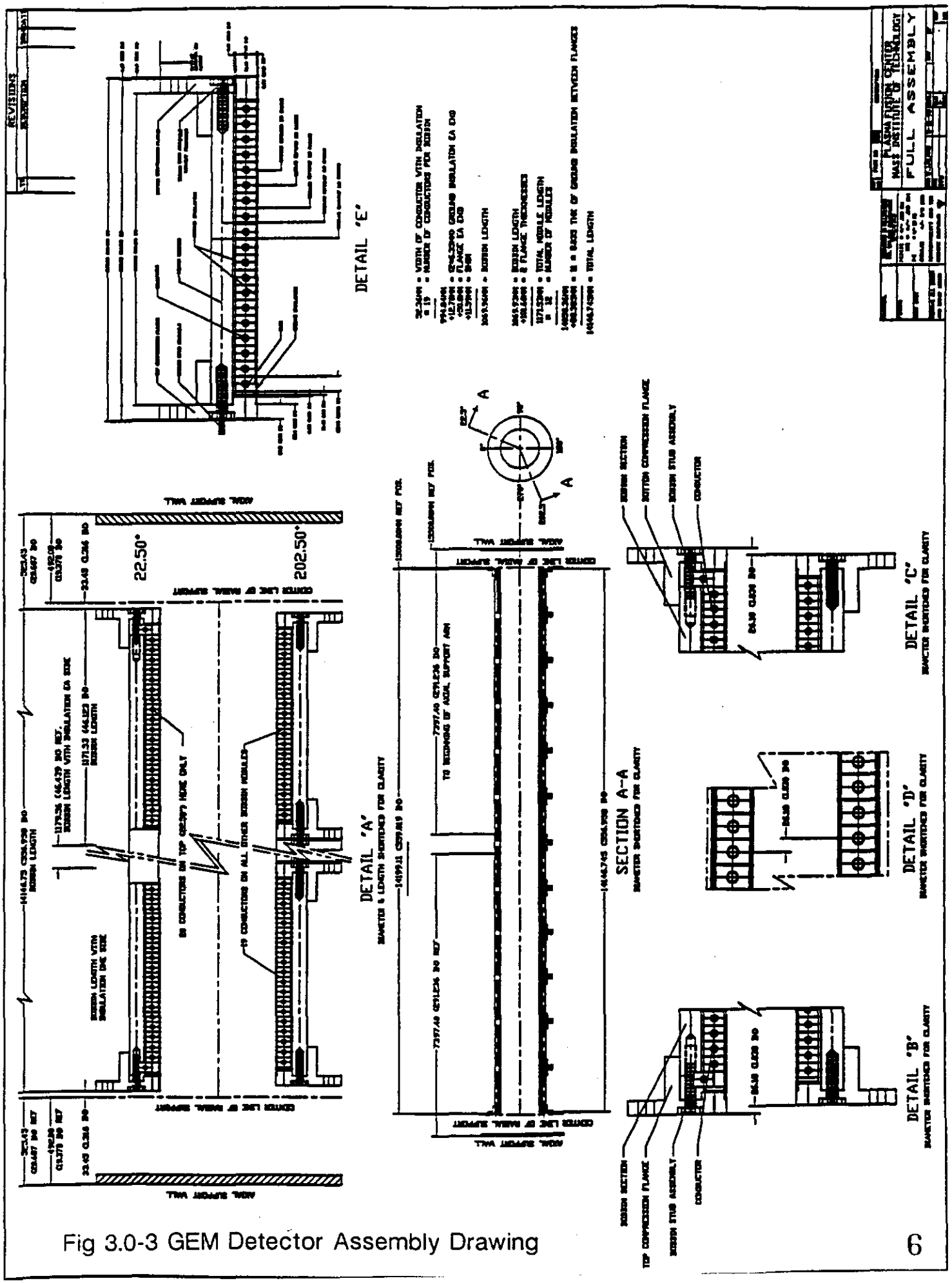

Fig 3.0-3 GEM Detector Assembly Drawing

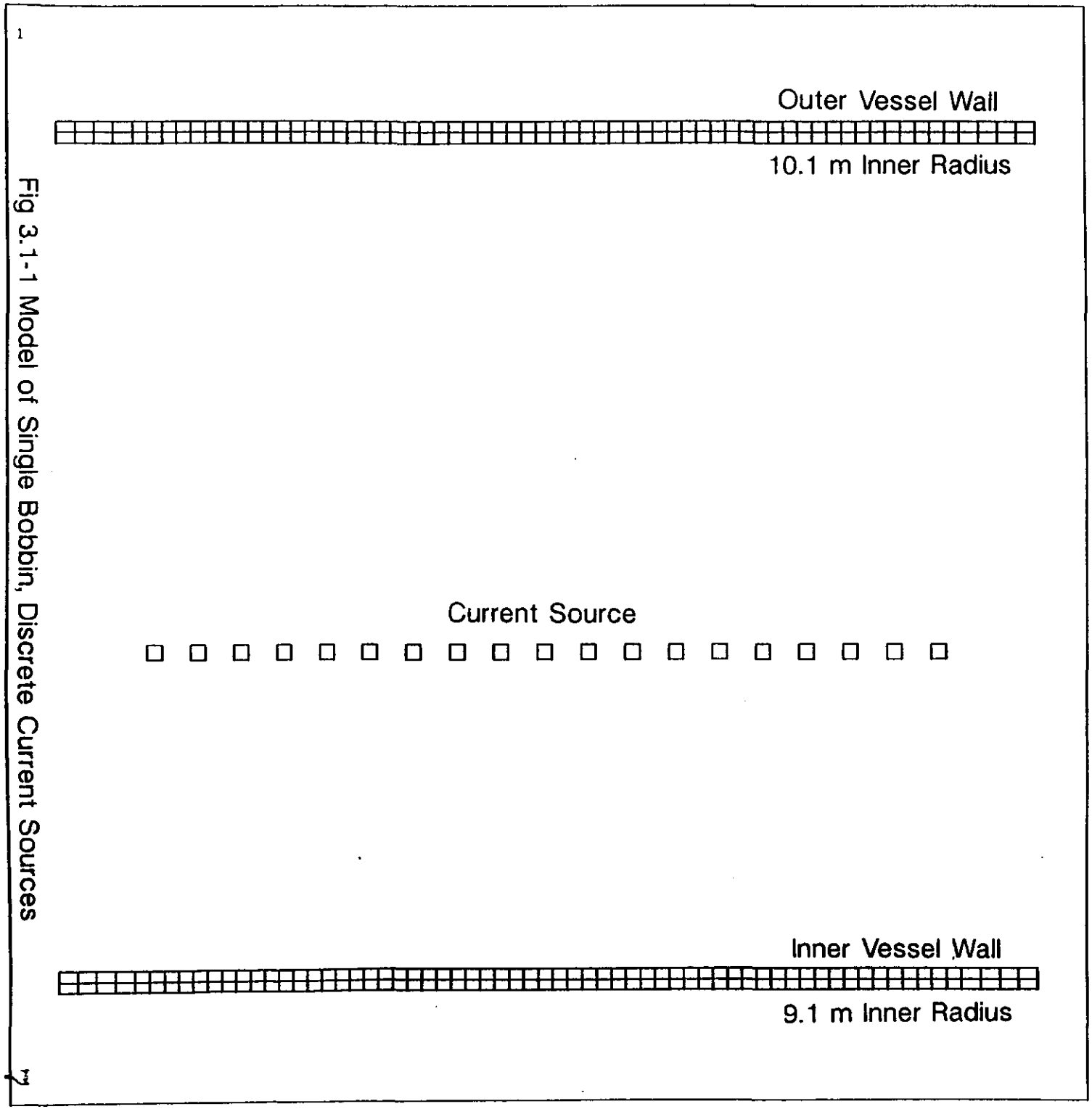

Fig 3.1-1 Model of Single Bobbin, Discrete Current Sources

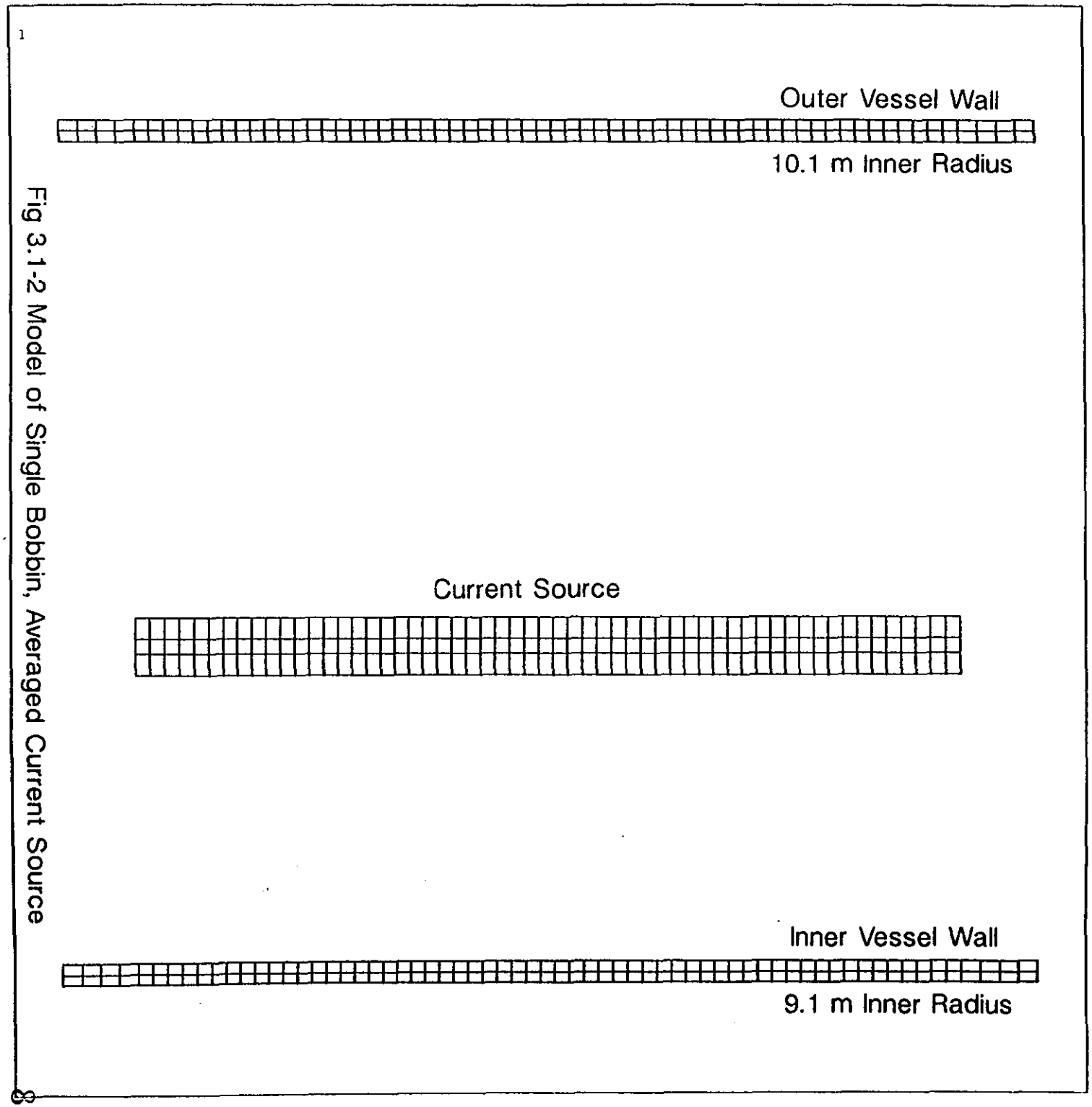

Fig 3.1-2 Model of Single Bobbin, Averaged Current Source

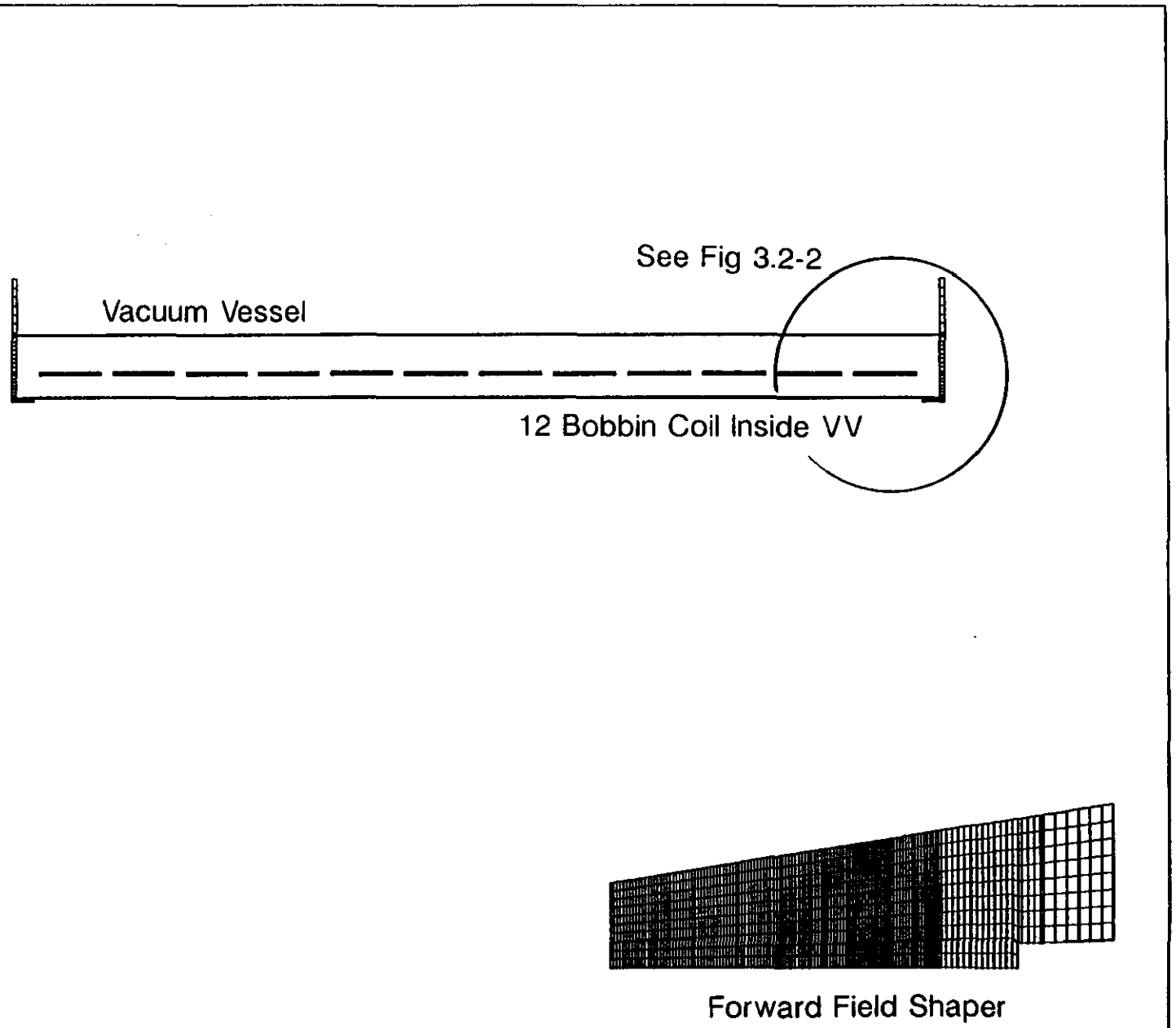

Fig 3.2-1 Model of GEM Detector Coil, FFS and Vacuum Vessel

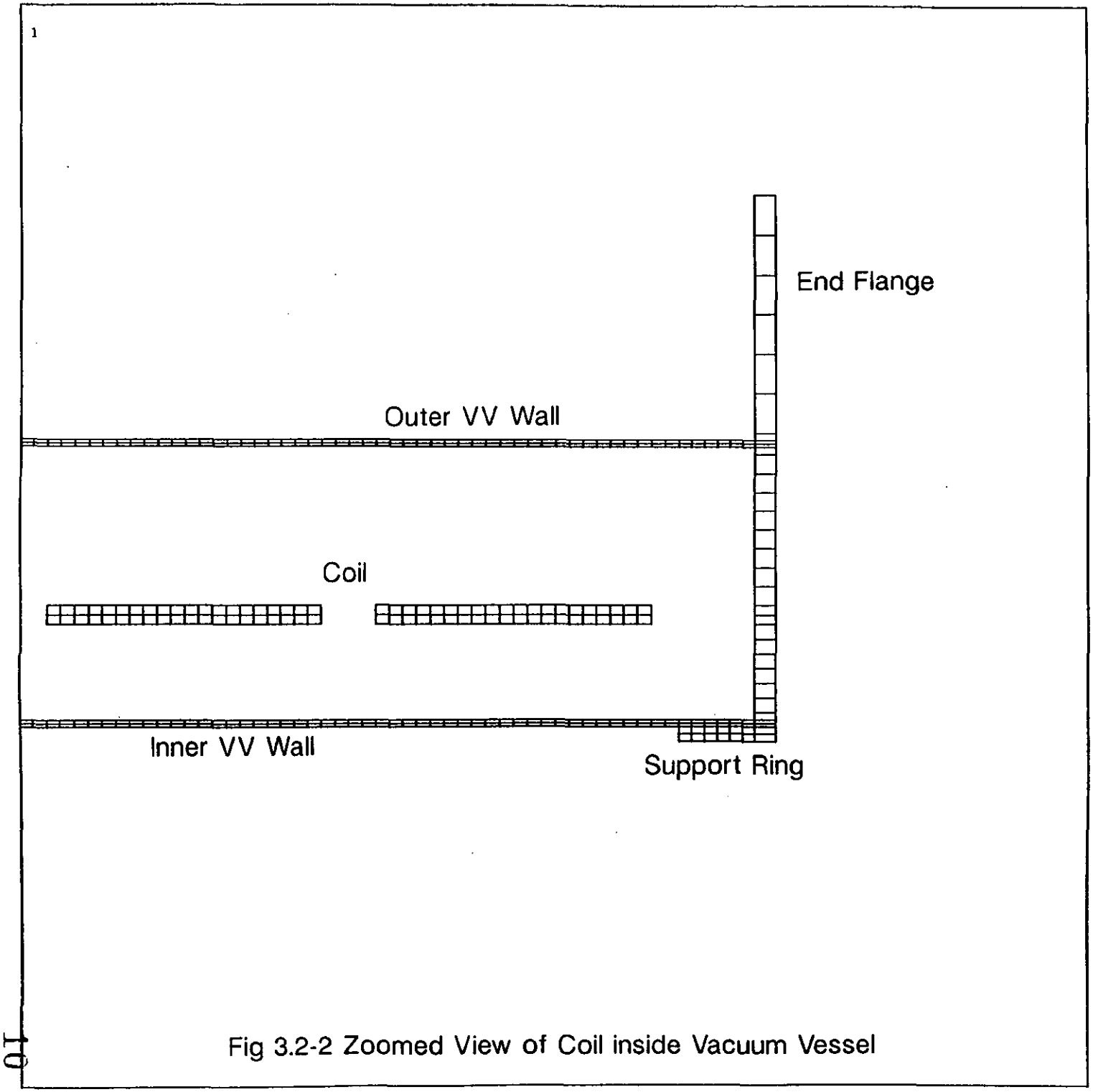

ANSYS 5.0
JUN 29 1993
16:13:38
PLOT NO. 1
ELEMENTS
MAT NUM

ZV =-1
*DIST=1.937
*XF =9.742
*YF =14.54
VUP =X

Fig 3.2-2 Zoomed View of Coil inside Vacuum Vessel

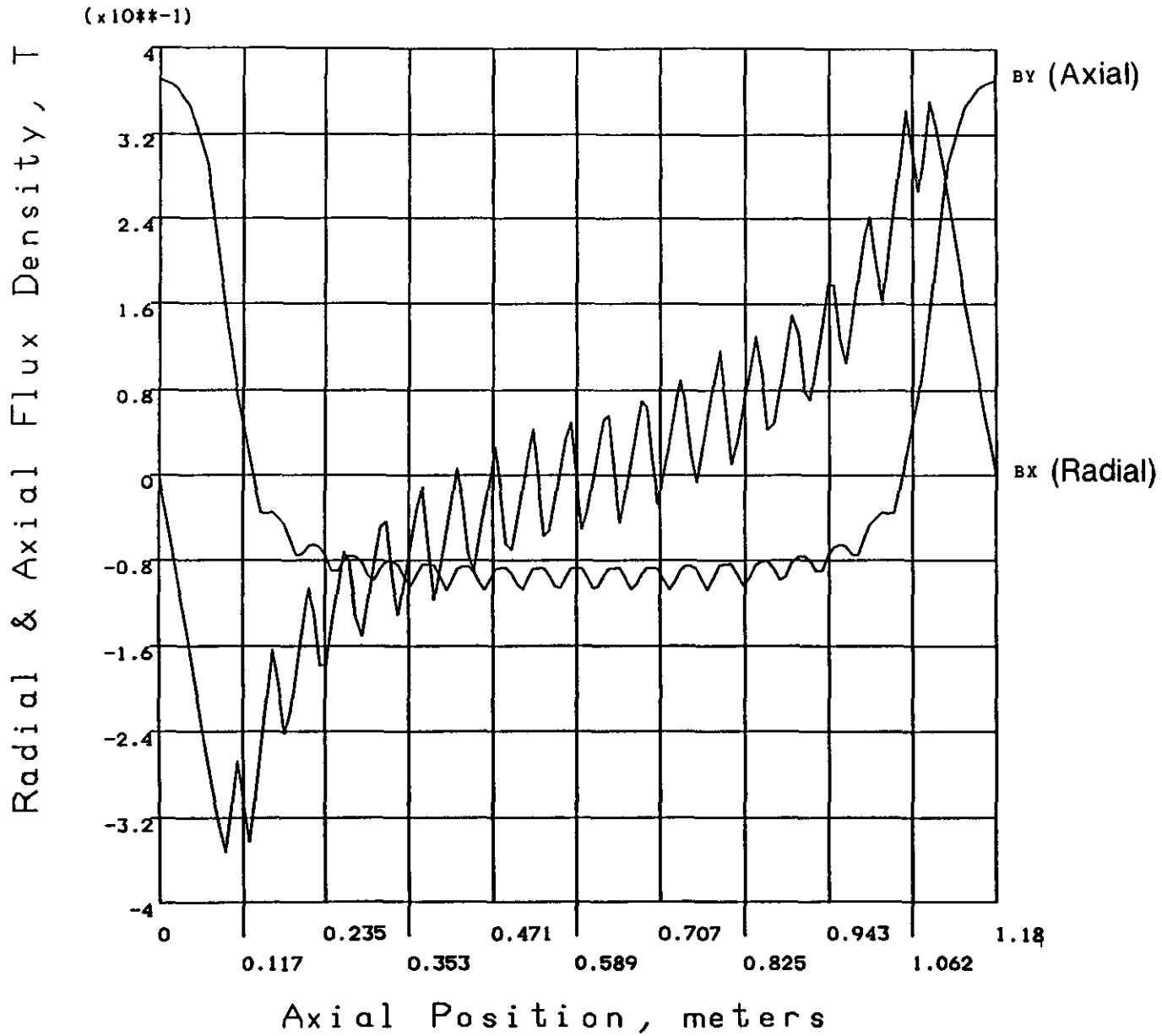

ANSYS 5.0
JUN 29 1993
16:51:26
PLOT NO. 2
POST1
STEP=2
SUB =1
TIME=2
PATH PLOT
NOD1=25
NOD2=3730

ZV =1
DIST=0.75
XF =0.5
YF =0.5
ZF =0.5

Fig 4.1-1 Flux Density Across Bobbin Width, R=9.534 m, 19 Current Sources

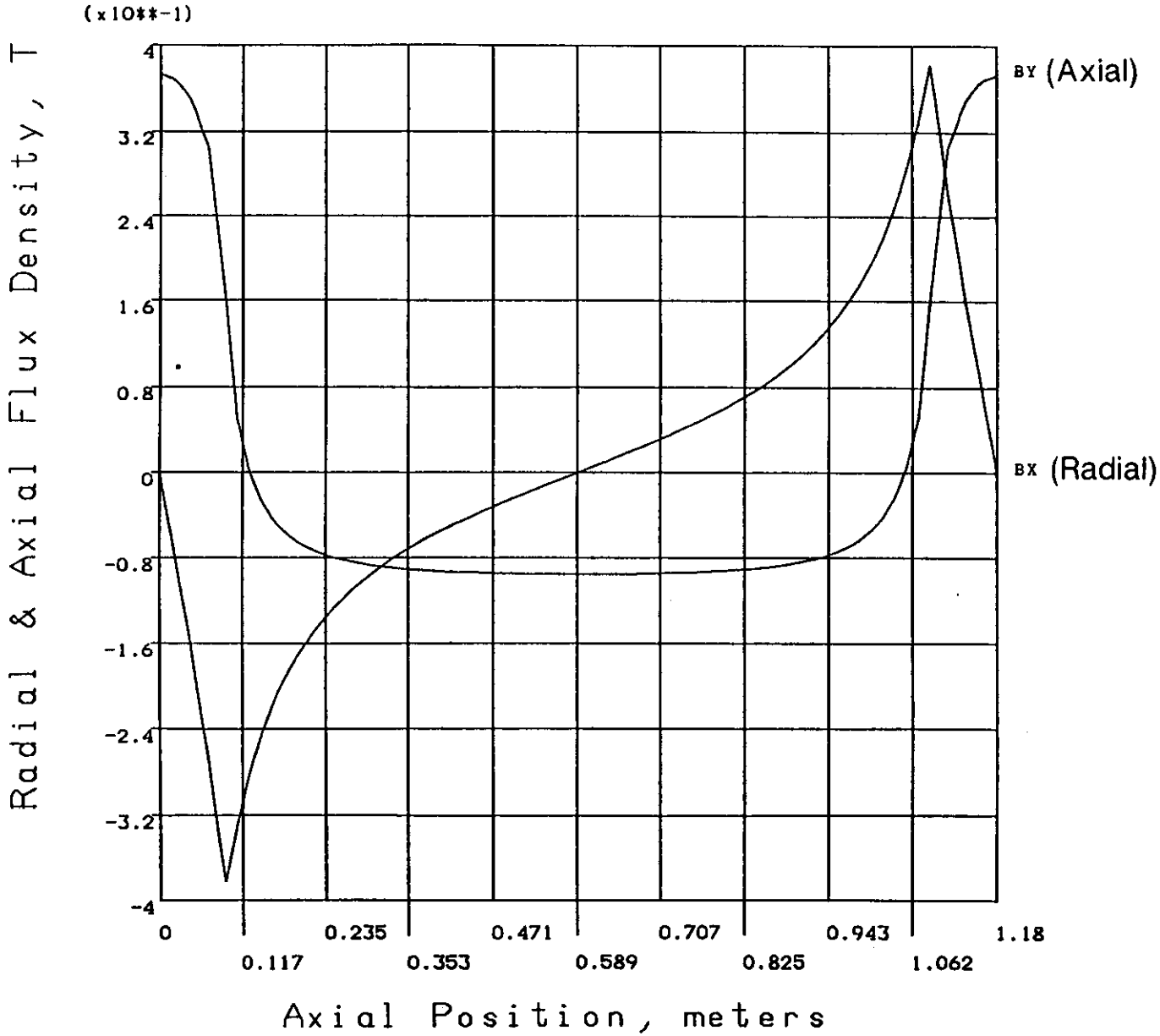

ANSYS 5.0
JUN 29 1993
16:25:55
PLOT NO. 2
POST1
STEP=2
SUB =1
TIME=2
PATH PLOT
NOD1=25
NOD2=3730

ZV =1
DIST=0.75
XF =0.5
YF =0.5
ZF =0.5

Fig 4.1-2 Flux Density Across Bobbin, R=9.534 m, Averaged Current Source

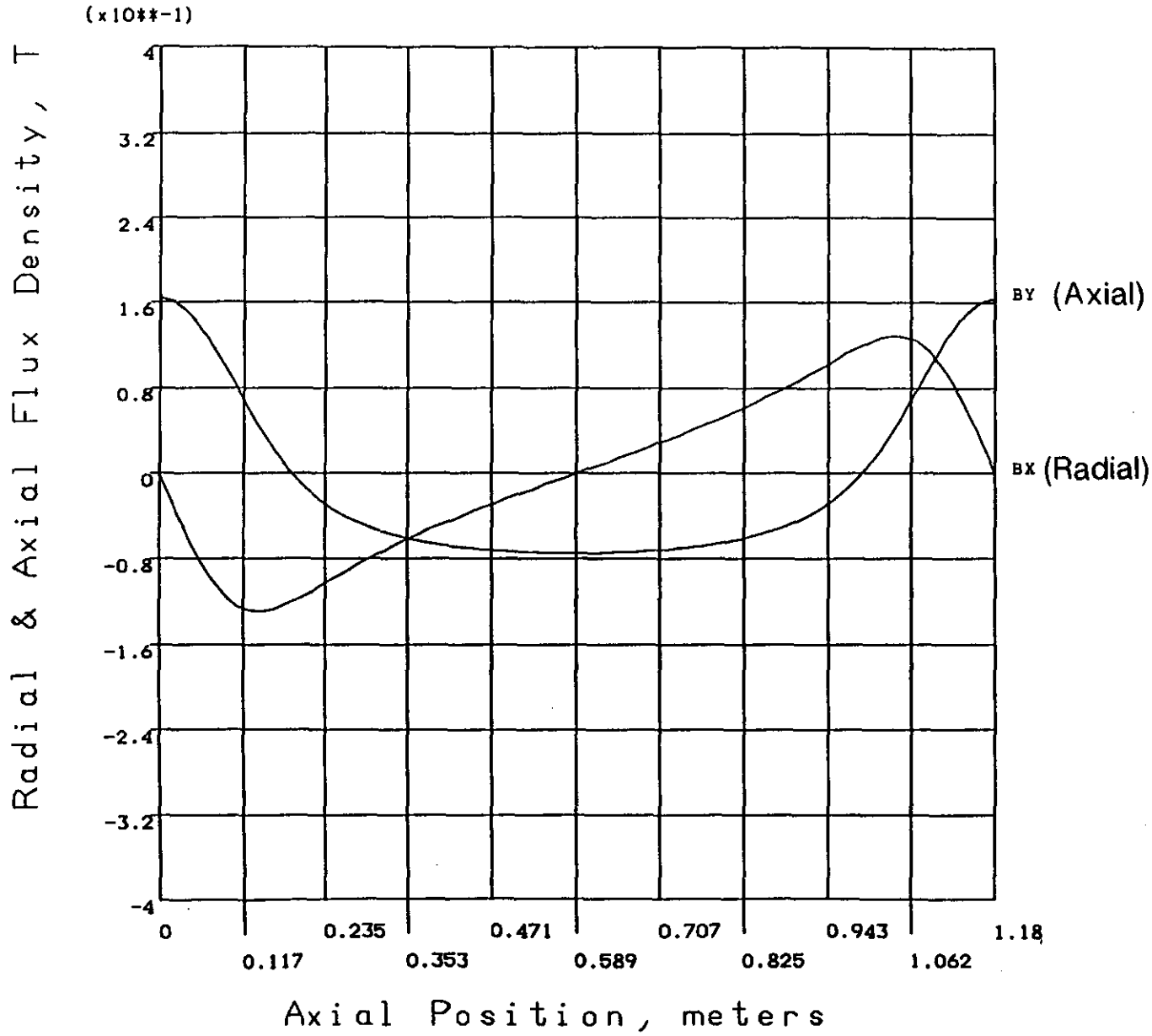

ANSYS 5.0
JUN 29 1993
16:53:15
PLOT NO. 5
POST1
STEP=2
SUB =1
TIME=2
PATH PLOT
NOD1=28
NOD2=3733

ZV =1
DIST=0.75
XF =0.5
YF =0.5
ZF =0.5

Fig 4.1-3 Flux Density Across Bobbin, R=9.617 m, 19 Current Sources

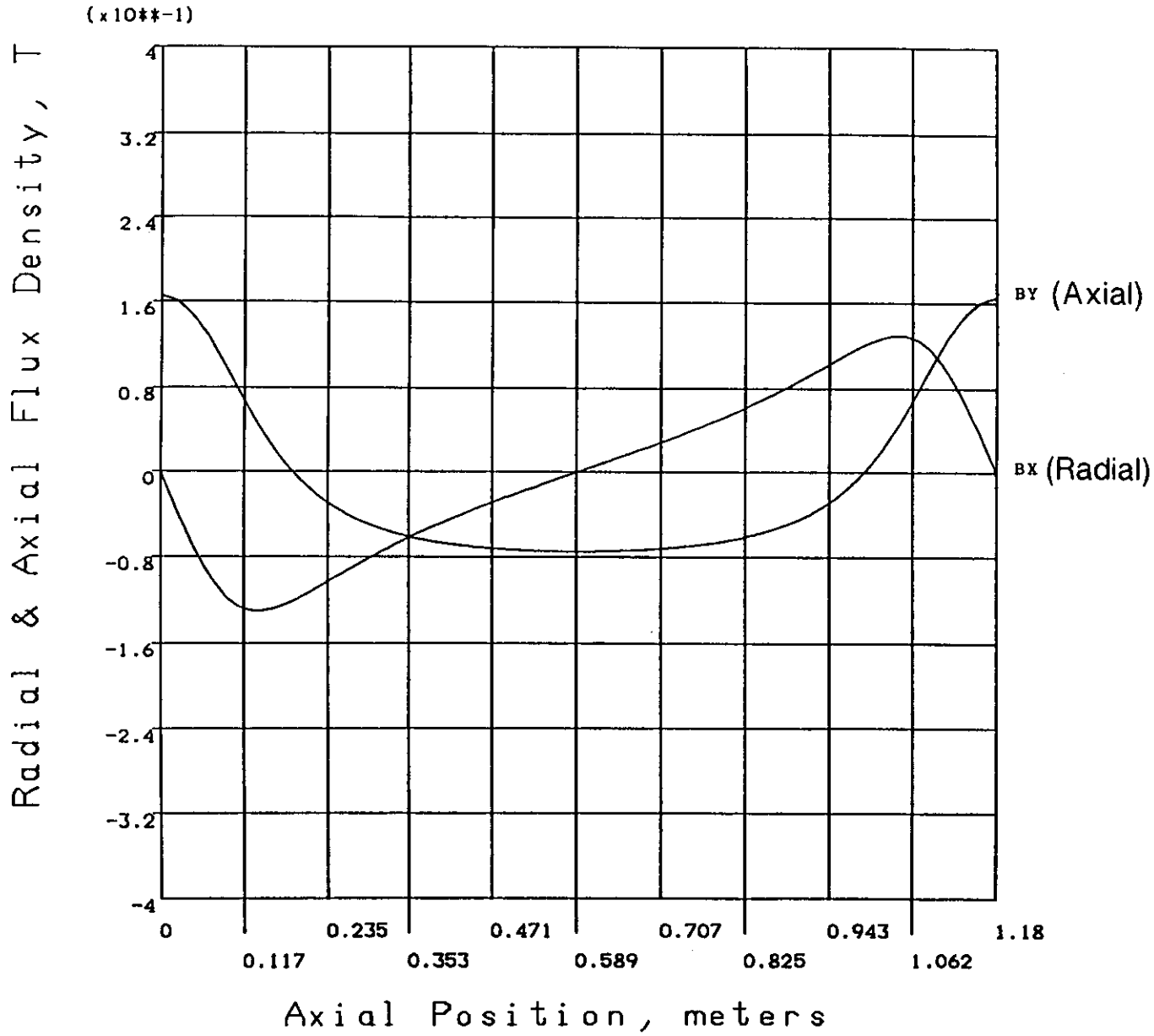

ANSYS 5.0
JUN 29 1993
16:27:45
PLOT NO. 5
POST1
STEP=2
SUB =1
TIME=2
PATH PLOT
NOD1=28
NOD2=3733

ZV =1
DIST=0.75
XF =0.5
YF =0.5
ZF =0.5

Fig 4.1-4 Flux Density Across Bobbin, R=9.617 m, Averaged Current Source

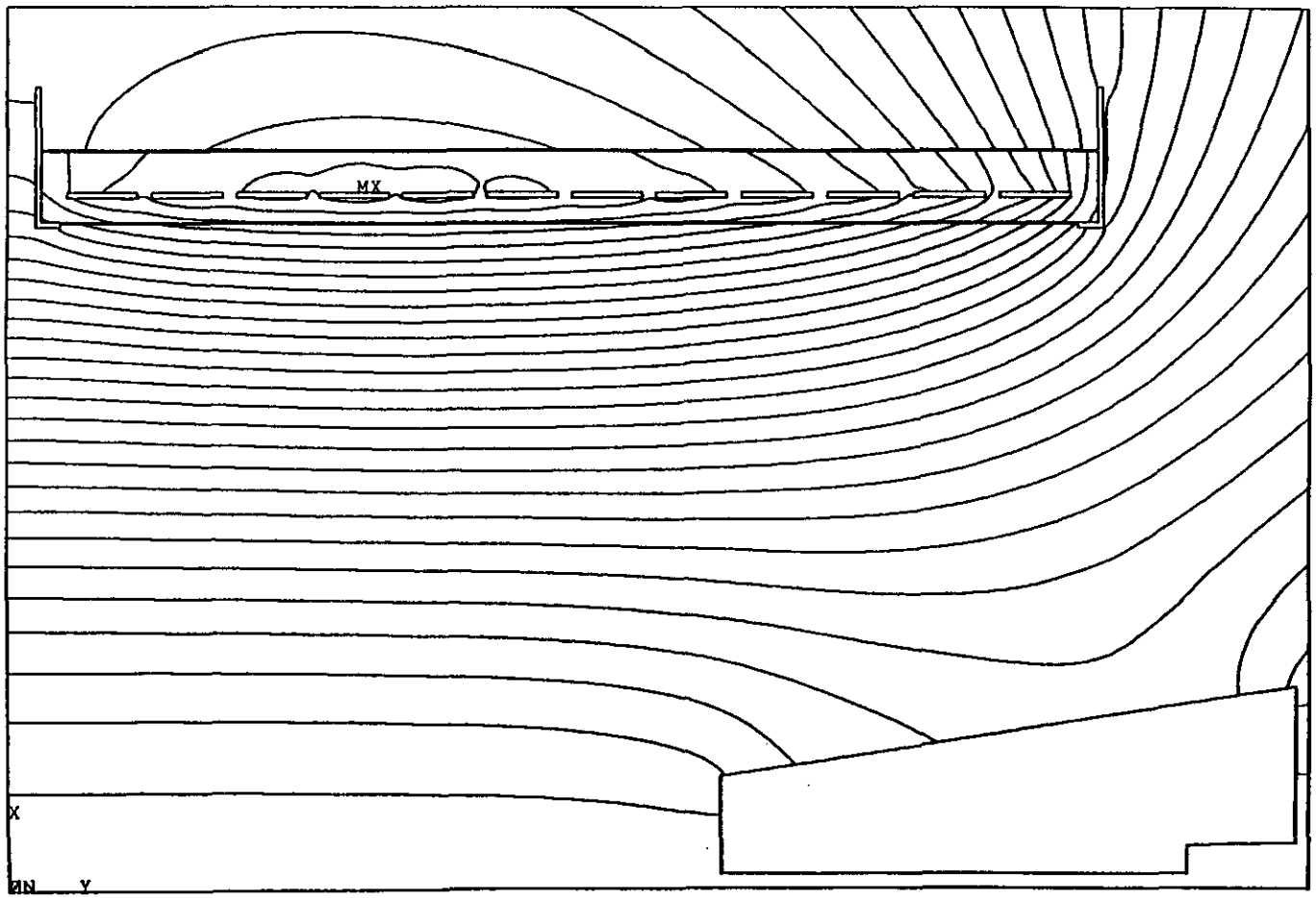

ANSYS 5.0
JUN 19 1993
10:22:01
PLOT NO. 1
NODAL SOLUTION
STEP=2
SUB =1
TIME=2
R*AZ
RSYS=0
SMX =38.279
0.708866
2.127
3.544
4.962
6.38
9.215
10.633
12.051
13.468
16.304
17.722
19.139
20.557
23.393
24.81
26.228
27.646
30.481
31.899
33.317
34.734
37.57

Fig 4.2-1 Axisymmetric Flux Contours

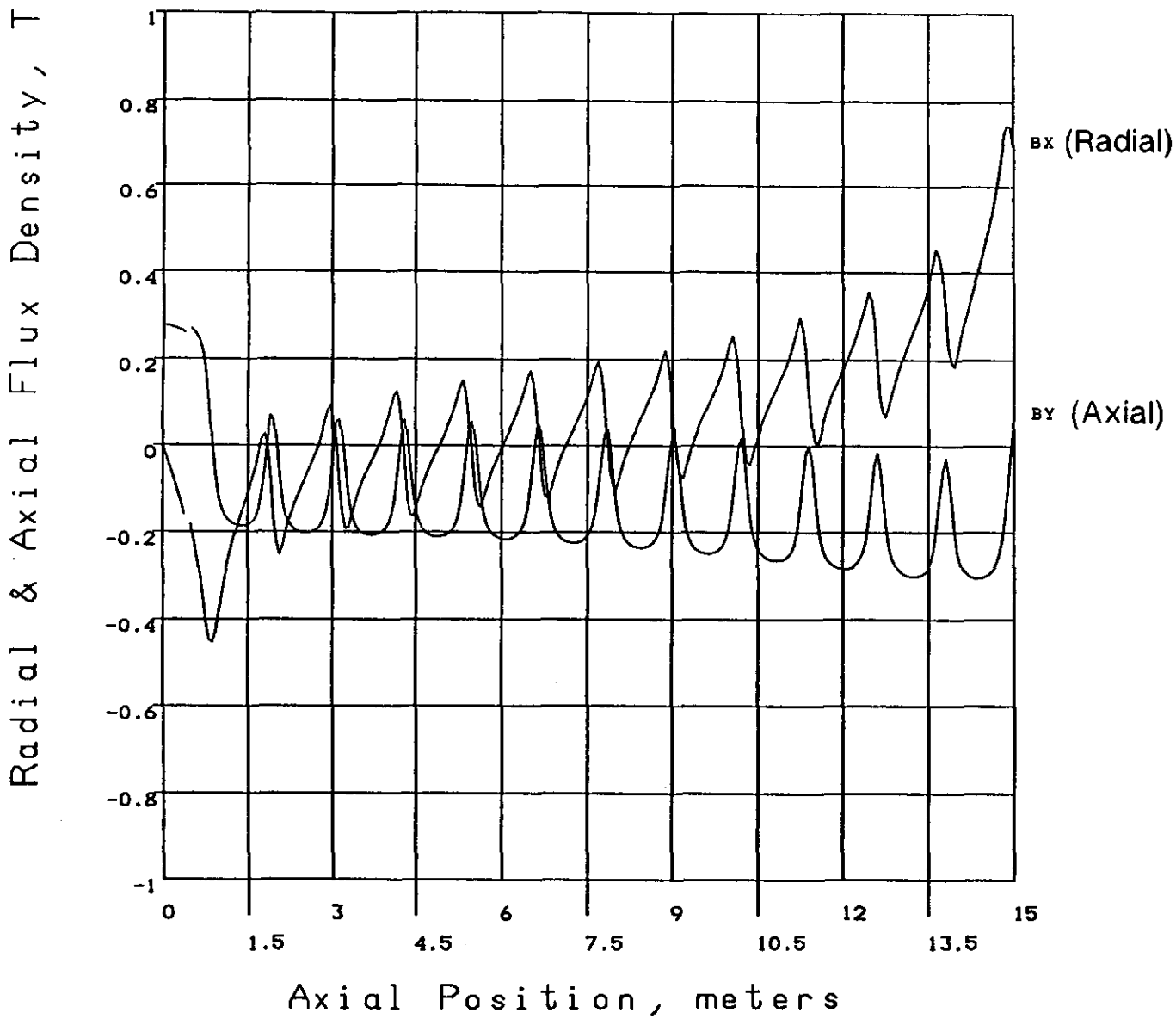

ANSYS 5.0
JUN 27 1993
13:38:07
PLOT NO. 2
POST1
STEP=2
SUB =1
TIME=2
PATH PLOT
NOD1=19552
NOD2=19852

ZV =1
DIST=0.75
XF =0.5
YF =0.5
ZF =0.5
EDGE

Fig 4.2-2 Flux Density Path Plot from Symmetry Plane to 15 m, R=9.602 m

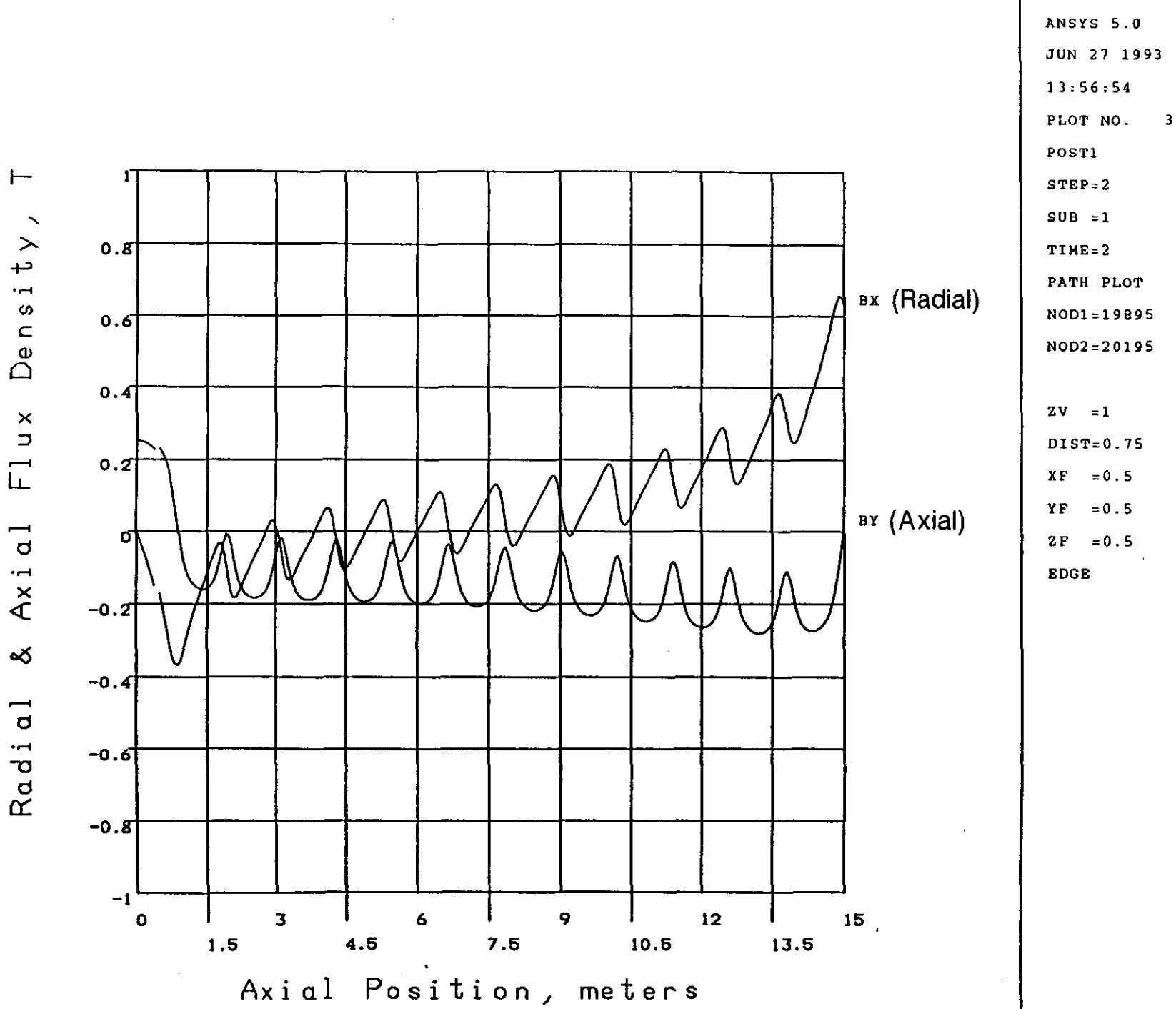

Fig 4.2-3 Flux Density Path Plot from Symmetry Plane to 15 m, R=9.669 m

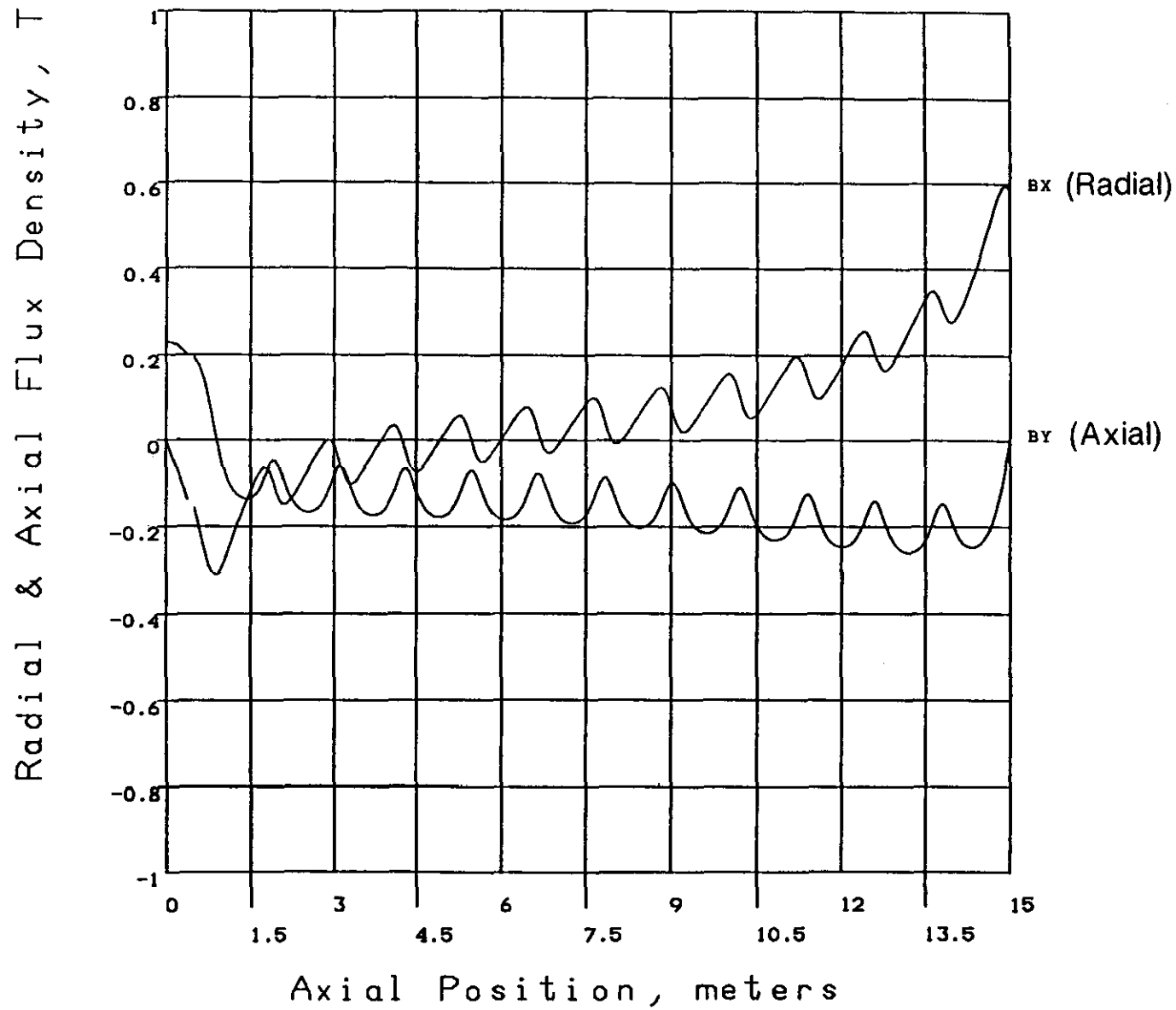

ANSYS 5.0
JUN 27 1993
14:15:33
PLOT NO. 4
POST1
STEP=2
SUB =1
TIME=2
PATH PLOT
NOD1=20238
NOD2=20538

ZV =1
DIST=0.75
XF =0.5
YF =0.5
ZF =0.5
EDGE

Fig 4.2-4 Flux Density Path Plot from Symmetry Plane to 15 m, R=9.737 m

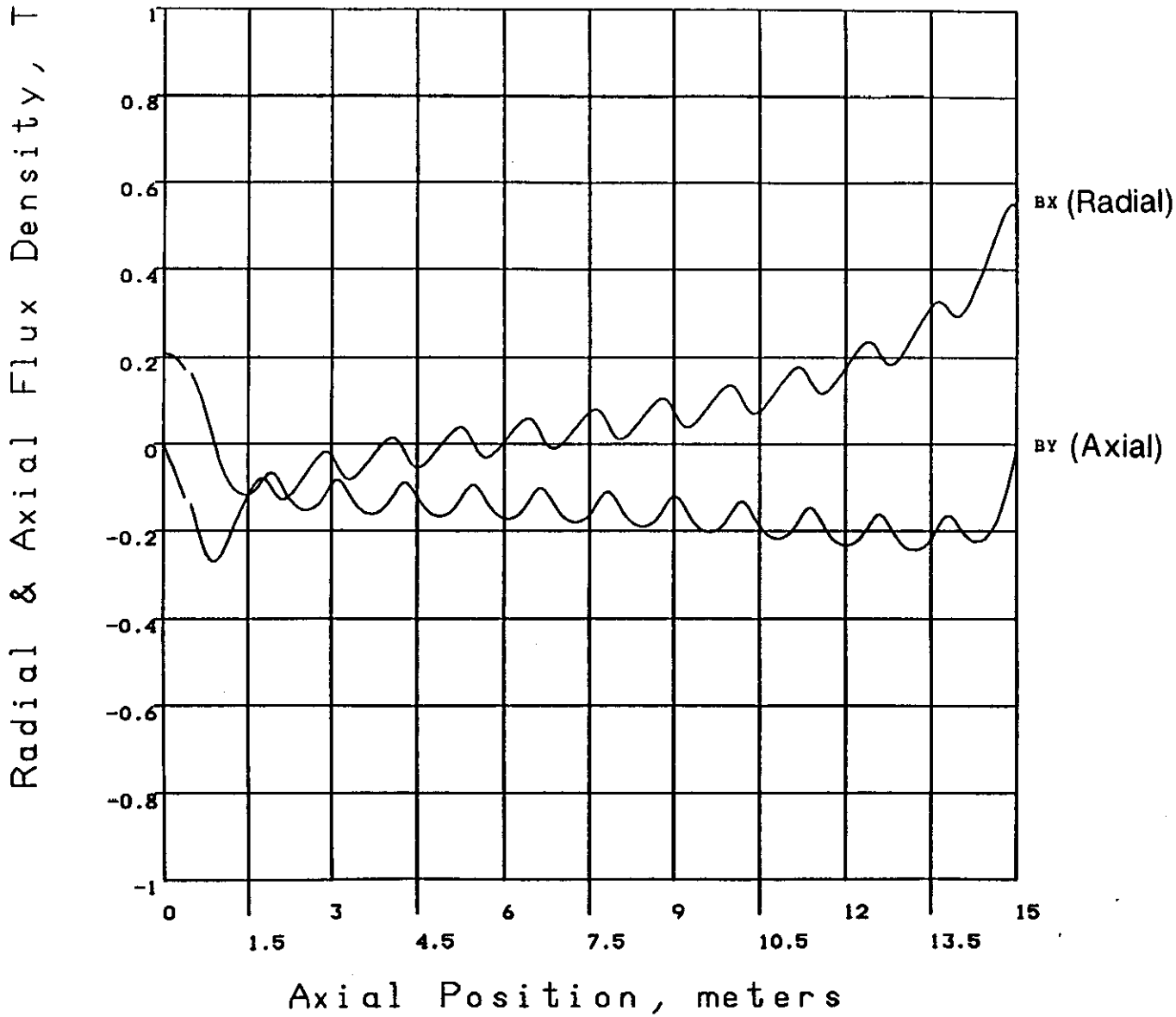

ANSYS 5.0
JUN 27 1993
14:34:21
PLOT NO. 5
POST1
STEP=2
SUB =1
TIME=2
PATH PLOT
NOD1=20581
NOD2=20881

ZV =1
DIST=0.75
XF =0.5
YF =0.5
ZF =0.5
EDGE

Fig 4.2-5 Flux Density Path Plot from Symmetry Plane to 15 m, R=9.804 m

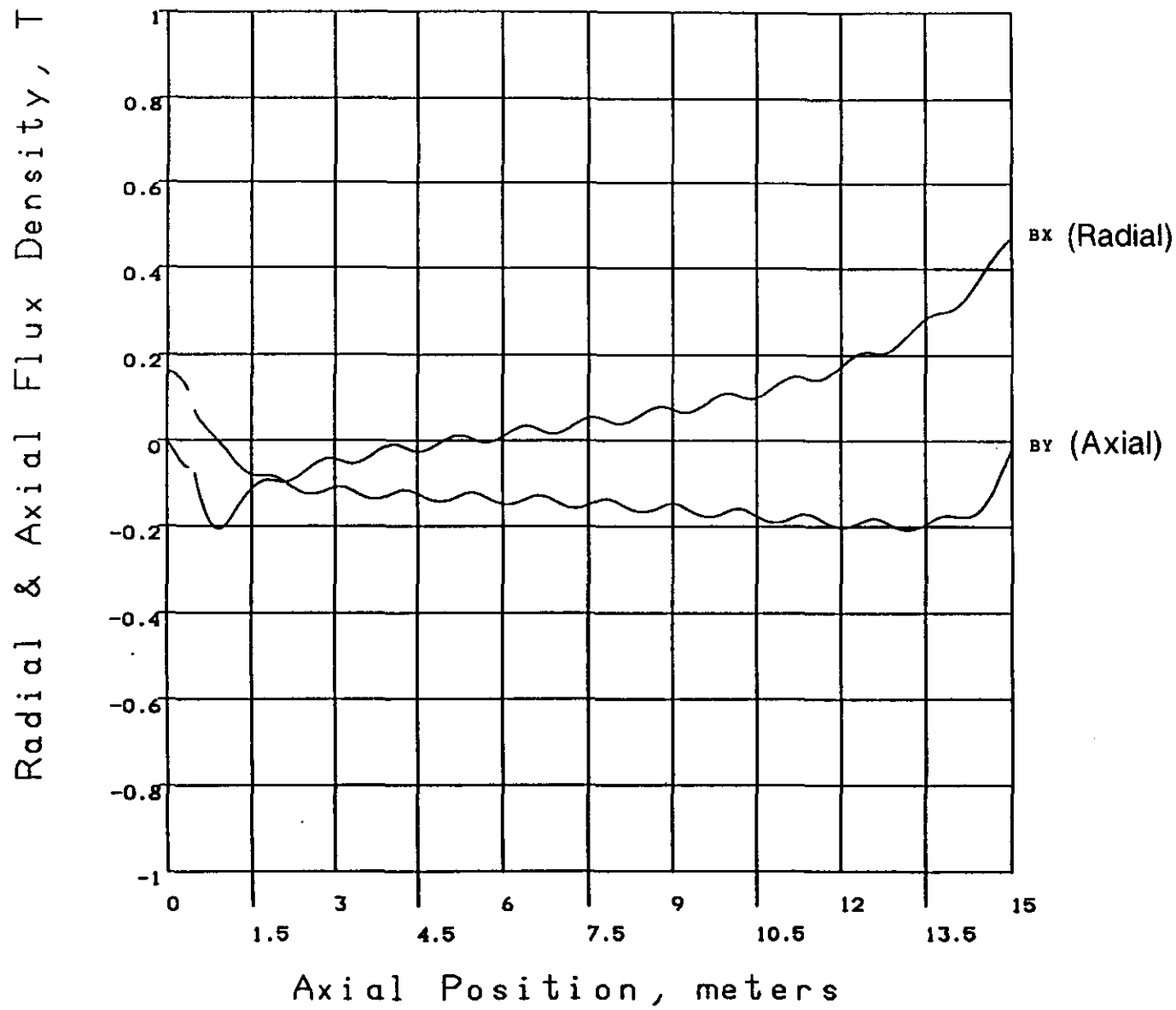

ANSYS 5.0
JUN 27 1993
15:29:55
PLOT NO. 8
POST1
STEP=2
SUB =1
TIME=2
PATH PLOT
NOD1=21610
NOD2=21910

ZV =1
DIST=0.75
XF =0.5
YF =0.5
ZF =0.5
EDGE

Fig 4.2-6 Flux Density Path Plot from Symmetry Plane to 15 m, R=10.007 m

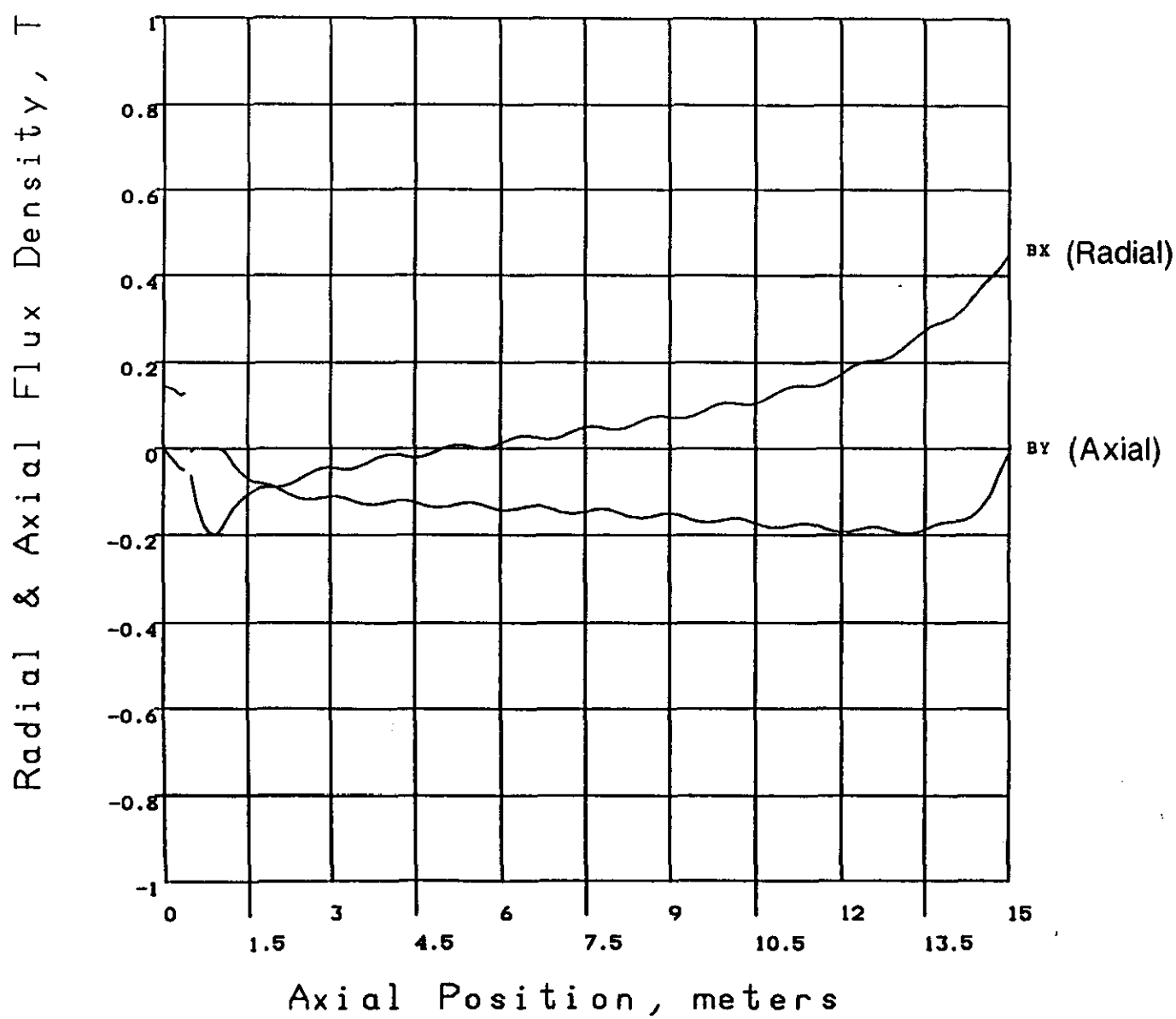

ANSYS 5.0
JUN 27 1993
16:07:09
PLOT NO. 10
POST1
STEP=2
SUB =1
TIME=2
PATH PLOT
NOD1=22296
NOD2=22596

ZV =1
DIST=0.75
XF =0.5
YF =0.5
ZF =0.5
EDGE

Fig 4.2-7 Flux Density Path Plot from Symmetry Plane to 15 m, R=10.100 m

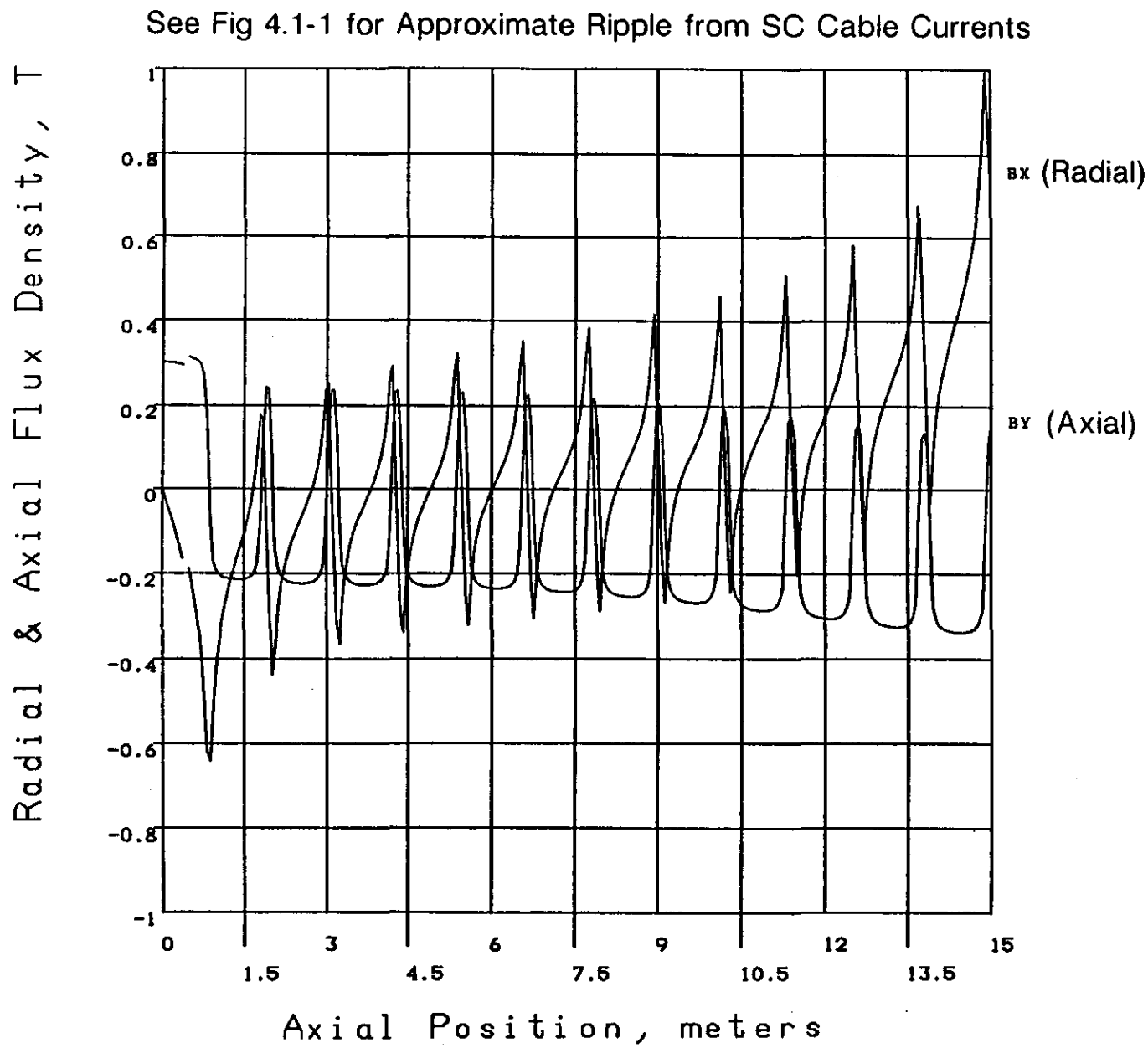

ANSYS 5.0
JUN 27 1993
13:19:44
PLOT NO. 1
POST1
STEP=2
SUB =1
TIME=2
PATH PLOT
NOD1=19209
NOD2=19509

ZV =1
DIST=0.75
XF =0.5
YF =0.5
ZF =0.5
EDGE

Fig 4.2-8 Flux Density Path Plot from Symmetry Plane to 15 m, R=9.534 m